Smart Structures and Systems, *Vol. 26, No. 3 (2020) 331-343*
DOI: https://doi.org/10.12989/sss.2020.26.3.331

Magneto-electro-elastic vibration analysis of modified couple stress-based three-layered micro rectangular plates exposed to multi-physical fields considering the flexoelectricity effects

Mohammad Khorasani [1], Arameh Eyvazian [2], Mohammed Karbon [2], Abdelouahed Tounsi*[3,4], Luca Lampani [1] and Tamer A. Sebaey [5,6]

[1] *Department of Mechanical and Aerospace Engineering, Sapienza University, Via Eudossiana 18, 00184, Rome, Italy*
[2] *Department of Mechanical and Industrial Engineering, Qatar University, P.O. Box 2713, Doha, Qatar*
[3] *Department of Civil and Environmental Engineering, King Fahd University of Petroleum & Minerals, 31261 Dhahran, Eastern Province, Saudi Arabia*
[4] *Material and Hydrology Laboratory, University of Sidi Bel Abbes, Faculty of Technology, Civil Engineering Department, Algeria*
[5] *Department of Mechanical Design and Production, Faculty of Engineering, Zagazig University, P.O. Box 44519, Zagazig, Sharkia, Egypt*
[6] *Department of Engineering Management, College of Engineering, Prince Sultan University, Riyadh, Saudi Arabia*

(*Received December 31, 2019, Revised April 10, 2020, Accepted April 11, 2020*)

Abstract. In this paper, based on the CPT, motion equations for a sandwich plate containing a core and two integrated face-sheets have derived. The structure rests on the Visco-Pasternak foundation, which includes normal and shear modules. The piezo-magnetic core is made of $CoFe_2O_4$ and also is subjected to 3D magnetic potential. Two face sheets at top and bottom of the core are under electrical fields. Also, in order to obtain more accuracy, the effect of flexoelectricity has took into account at face sheets' relations in this work. Flexoelectricity is a property of all insulators whereby they polarize when subject to an inhomogeneous deformation. This property plays a crucial role in small-scale rather than macro scale. Employing CPT, Hamilton's principle, flexoelectricity considerations, the governing equations are derived and then solved analytically. By present work a detailed numerical study is obtained based on Piezoelectricity, Flexoelectricity and modified couple stress theories to indicate the significant effect of length scale parameter, shear correction factor, aspect and thickness ratios and boundary conditions on natural frequency of sandwich plates. Also, the figures show that there is an excellent agreement between present study and previous researches. These finding can be used for automotive industries, aircrafts, marine vessels and building industries.

Keywords: flexoelectricity; vibration analysis; sandwich plates; modified couple stress theory; electro-magnetic fields

1. Introduction

The past decade has witnessed the successful development of micro/nano-electro-mechanical systems (MEMS/NEMS) like piezoelectric-gated diodes, resonators (Tanner *et al*. 2007), generators (Wang 2006), mechanical sensors (Lao *et al*. 2007, Zhang *et al* 2015) and energy harvesters according to demand of high precision and wireless NEMS devices. Using these applications of piezoelectric and piezomagnetic nanostructures, necessitates scholars to have a profound understanding of the electro-mechanical and magneto-mechanical coupling behaviors of piezoelectric and piezomagnetic materials at the nano/micro-scale. The magnetoelectric effect is electric polarization due to an external magnetic field and magnetization due to the electric field. By using this important effect, scientists are able to control magnetic properties of a material by using electric field and vice versa. So, moving the borders of knowledge about magnetoelectric structures seems to be essential. For this reason, as an example, Kiran and Kattimani (2018) researched on Free vibration of FGSMEE plates. They used finite element model to investigate the effect of power-law gradient, thickness ratio, boundary conditions and aspect ratio on the free vibration and static response characteristics of FGSMEE plate. As another attempt, Mahesh *et al*. (2019) addresses the coupled free vibration problem of skew magneto-electro-elastic plates (SMEE). They consider the temperature-moisture dependent material properties in their study and reveal that the external environment as well as the geometrical skewness has a significant influence on the stiffness of the SMEE plates.

Piezoelectricity serves the linear response of polarization to mechanical strain and vice versa. This phenomenon is possible only in non-centrosymmetric materials. Beside piezoelectric, the flexoelectric is a coupling between polarization and strain gradient, rather than between polarization and homogeneous strain. Having a perfect understanding of this frail difference is necessary to understand advantages and the limitations of flexoelectricity relative to piezoelectricity. As another expression, piezoelectricity represents the linear coupling between electrical and mechanical variables while,

*Corresponding author, Professor,
E-mail: abdelouahed.tounsi@univ-sba.dz;
tou_abdel@yahoo.com

ISSN: 1738-1584 (Print), 1738-1991 (Online)

flexoelectricity denotes the linear coupling between strain gradient and polarization (Yudin and Tagantsev 2013) and strain and polarization gradient (Mindlin 1968). It is also worthwhile mentioning that analogous to definitions of the direct and the converse piezoelectric effects, induction of the electric polarization due to the strain gradient has called direct flexoelectric effect and increasing mechanical stress or strain due to the electric field gradient has termed converse flexoelectric effect. Based on statistics, it has revealed that flexoelectric effect is more significant in micro and nano-scale.

In the past century, a lot of studies have done by different researchers to provide more clear understanding about vibrational, buckling and bending behaviors of different Piezoelectric and functionally graded shells and plates. As first example, Duc and Thang (2014) used an analytical approach to investigate the nonlinear static buckling for imperfect eccentrically stiffened FG thin circular cylindrical shells. In the same year, transient responses of FG double curved shallow shells with temperature-dependent material properties in thermal environment has examined by Duc and Quan (2014). After that, Duc *et al*. (2015) evaluated mechanical and thermal stability of eccentrically stiffened functionally graded conical shell panels resting on elastic foundations in thermal environment. Furthermore, Duc *et al*. (2017a) elaborated on nonlinear dynamic response and vibration of imperfect eccentrically stiffness functionally graded elliptical cylindrical shells on elastic foundations using both the classical shell theory (CST) and Airy stress functions method with motion equations using Volmir's assumption. Moreover, based on Reddy's third-order shear deformation shell theory, Duc *et al*. (2017b) and Khoa *et al*. (2017) presented an analytical approach to investigate the nonlinear thermo-mechanical response and nonlinear buckling and postbuckling response of imperfect Sigmoid FGM circular cylindrical shells surrounded on elastic foundations, respectively. More recently, nonlinear thermomechanical buckling and post-buckling response of porous FGM plates have investigated using Reddy's HSDT by Cong *et al*. (2018). Also, the stability in a rectangular functionally grade material (FGM) plate with central crack studied by Minh and Duc (2019)

On the other hand, theoretical work on flexoelectricity dates back to 1957, where Mashkevich (1957) proposed the effect of flexoelectricity for the first time. After that, Kogan formulated this phenomenon. Kogan estimated the flexoelectric coefficients for crystal dielectrics with order of $\frac{e}{a} = 10^{-9} c/m$, where e is the electron charge, and a is the lattice parameter Sharma *et al*. (2007). Tagantsev (1986) theoretically confirmed that the flexoelectric effect in the crystalline solids is different from the piezoelectric effect and he derived a simple model for computing the flexoelectric coefficients. Experimental researches of the converse flexoelectric effect due to the inhomogeneous electric field in barium strontium were conducted by Fu *et al*. (2006). Moreover, Maranganti *et al*. (2006) developed a variation principle for dielectrics including both the strain gradient and polarization gradient effects. Then a lot of experiments have done by (Ma and Cross 2001, 2002, 2006) to examine the flexoelectricity quantitatively, by measuring the flexoelectric coefficients of ferroelectric ceramics. In recent years, efforts have made by researchers to provide perfect understanding on this fragile effect by investigation of experimental and theoretical results. For example, possible applications of the flexoelectricity in solids has conducted by Zubko *et al*. (2013). After that, a thorough and comprehensive review of the physical fundamentals has done by Nguyen *et al*. (2013). Also, in 2013, Yudin and Tagantsev (2013) presented a critical analysis of the knowledge on the flexoelectricity in common solids, excluding organic materials and liquid crystals. The influence of flexoelectricity on the electromechanical coupling behavior of a piezoelectric nanoplate surveyed by Yang *et al*. (2015). They hired Kirchhoff plate theory and Hamilton's principle to derive their results. Also, size dependency of flexoelectric effect has revealed using simulation results on the electroelastic fields. After that, Barati (2017) examined Coupled effects of electrical polarization-strain gradient on vibration behavior of double-layered flexoelectric nanoplates and he succeed to prove that flexoelectricity yields a considerable difference between his model and previous investigations on conventional piezoelectric nanoplates.

Separated from abovementioned efforts, some papers have studied in order to have complete mindset about different plate related theories. For instance, Batou *et al*. (2019) studied wave propagations in sigmoid functionally graded (S-FG) plates using new higher shear deformation theory (HSDT) based on two-dimensional (2D) elasticity theory. Beside this, Thu and Duc (2016), focused on non-linear dynamic response and vibration of an imperfect three-phase laminated nanocomposite cylindrical panel. They utilized HSDT in order to define displacement field in their paper. Duc and Tung (2010) and Duc and Cong (2015) conducted an analytical approach to investigating the stability of simply supported rectangular functionally graded plates and analytical approach to investigate the nonlinear dynamic response and vibration of thick functionally graded material (FGM) plates, respectively, using FSDT. Moreover, a simple four-variable integral plate theory is employed for examining the thermal buckling properties of functionally graded material (FGM) sandwich plates by Salah *et al*. (2019).

Finally, providing a through and comprehensive vibrational study on smart sandwich plates, with lighter and stiffer structure, in order to use in different and sensitive industries became a great motivation to conduct recent research. Therefore, using previous woks' contents, in this article we derive the governing equations of motion for a sandwich plate including a Piezomagnetic core and two flexoelectric face sheets based on classical and modified couple stress theories (CPT & MCST). The governing equations of motion are derived and solved by using Hamilton's principle. The results of this study investigate the effect of important parameters on vibrational behavior of sandwich flexoelectric plates. It is worthwhile mentioning that, Flexoelectric consideration for deriving governing equations is most important novelty of this paper. Moreover, such current sandwich model with different

boundary condition has not taken into vibrational examination yet.

2. Sandwich plate modeling

A sandwich plate including a piezomagnetic core, subjected to magnetic field, between two flexoelectric face sheets exposed to electric fields with length a, width b and thickness h resting on visco-Pasternak elastic foundation is shown in Fig. 1. Also, h_c is the thickness of central piezomagnetic core and h_t and h_b are the thickness of top and bottom flexoelectric face sheets, respectively, which $h = h_t + h_c + h_b$. Piezomagnetic core is made of polymer matrix and uniformly distributed CNT fibers. A Cartesian coordinate system (x, y, z) is used to describe the plate with the z-axis being along the thickness direction and the $x-y$ plane sitting on the mid-plane of plate. Both magnetic and electric fields assume to be along z direction. Because of simplicity and pursue aforementioned sandwich plate analyzation, it seems to be better to decompose problem to three separate portions (Piezomagnetic core, Flexoelectric face sheets and MCST). Then, related equations to each part should be presented. At the end, strain and kinetic energies of each part can be obtained using CPT. The total energy of sandwich plate is the sum of each part's energy.

In this research, CPT is utilized to model displacement fields for simplicity. Based on this theory, the displacements of an arbitrary point in the sandwich plate for both flexoelectric face sheets and piezo-magnetic core can be denoted as Wattanasakulpong and Chaikittiratana (2015)

$$\tilde{u}(x,y,z,t) = u(x,y,t) - zw_{,x}, \tag{1}$$

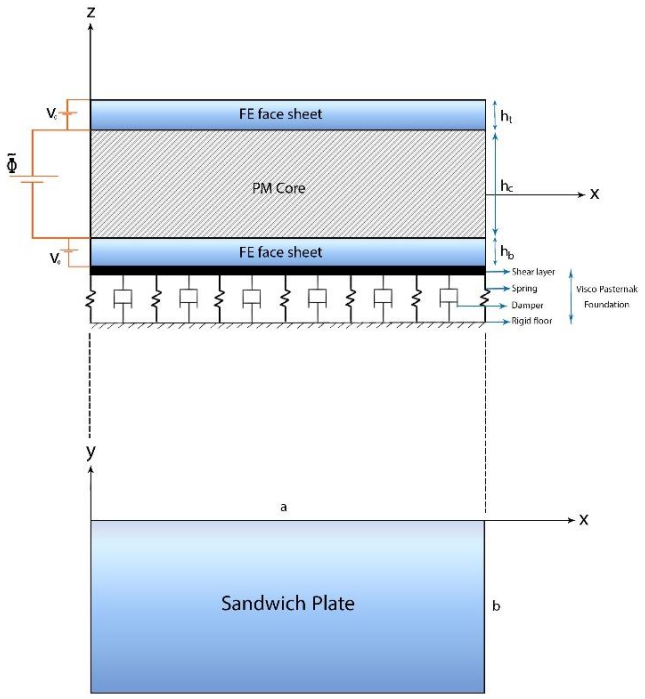

Fig. 1 2D Schematics of rectangular sandwich plate with Flexoelectric (FE) face sheets and Piezomagnetic (PM) core exposed to external magnetic and electric fields resting on Visco Pasternak foundation

$$\tilde{v}(x,y,z,t) = v(x,y,t) - zw_{,y}, \tag{2}$$

$$\tilde{w}(x,y,z,t) = w(x,y,t), \tag{3}$$

where u, v and w are the displacement components along the x, y and z directions, respectively.

2.1 Piezomagnetic core

Piezomagnetic core is made of $CoFe_2O_4$. As mentioned in section 2, the sandwich plate is containing a piezomagnetic core which is under magnetic field. In this section, the stress, strain and magnetic field relations for piezomagnetic core are derived. The strains can be obtained as Jafari Mehrabadi (2012)

$$\varepsilon_{xx}{}^{c} = \frac{\partial \tilde{u}}{\partial x} \tag{4}$$

$$\varepsilon_{yy}{}^{c} = \frac{\partial \tilde{v}}{\partial y} \tag{5}$$

$$\varepsilon_{xy}{}^{c} = \frac{1}{2}\left(\frac{\partial \tilde{u}}{\partial y} + \frac{\partial \tilde{v}}{\partial x}\right) \tag{6}$$

$$\varepsilon_{xz}{}^{c} = \frac{1}{2}\left(\frac{\partial \tilde{u}}{\partial z} + \frac{\partial \tilde{w}}{\partial x}\right) \tag{7}$$

$$\varepsilon_{yz}{}^{c} = \frac{1}{2}\left(\frac{\partial \tilde{v}}{\partial z} + \frac{\partial \tilde{w}}{\partial y}\right) \tag{8}$$

Where, superscript c represents piezomagnetic core. The stresses and magnetic induction can be presented as fallows Ebrahimi *et al*. (2019a)

$$\begin{bmatrix}\sigma_{xx}{}^{c}\\ \sigma_{yy}{}^{c}\\ \sigma_{xy}{}^{c}\\ \sigma_{yz}{}^{c}\\ \sigma_{xz}{}^{c}\end{bmatrix} = \begin{bmatrix}Q_{11} & Q_{12} & 0 & 0 & 0\\ Q_{12} & Q_{22} & 0 & 0 & 0\\ 0 & 0 & Q_{66} & 0 & 0\\ 0 & 0 & 0 & k_f Q_{44} & 0\\ 0 & 0 & 0 & 0 & k_f Q_{55}\end{bmatrix}\begin{bmatrix}\varepsilon_{xx}{}^{c}\\ \varepsilon_{yy}{}^{c}\\ 2\varepsilon_{xy}{}^{c}\\ 2\varepsilon_{yz}{}^{c}\\ 2\varepsilon_{xz}{}^{c}\end{bmatrix} + \begin{bmatrix}0 & 0 & r_{31}\\ 0 & 0 & r_{31}\\ 0 & 0 & 0\\ 0 & r_{24} & 0\\ r_{15} & 0 & 0\end{bmatrix}\begin{bmatrix}\frac{\partial}{\partial x}\tilde{\Phi}(x,y,z,t)\\ \frac{\partial}{\partial y}\tilde{\Phi}(x,y,z,t)\\ \frac{\partial}{\partial z}\tilde{\Phi}(x,y,z,t)\end{bmatrix}, \tag{9}$$

$$\begin{bmatrix}B_x\\ B_y\\ B_z\end{bmatrix} = \begin{bmatrix}0 & 0 & 0 & 0 & r_{15}\\ 0 & 0 & 0 & r_{24} & 0\\ r_{31} & r_{31} & 0 & 0 & 0\end{bmatrix}\begin{bmatrix}\varepsilon_{xx}{}^{c}\\ \varepsilon_{yy}{}^{c}\\ 2\varepsilon_{xy}{}^{c}\\ 2\varepsilon_{yz}{}^{c}\\ 2\varepsilon_{xz}{}^{c}\end{bmatrix} - \begin{bmatrix}\mu_{11} & 0 & 0\\ 0 & \mu_{22} & 0\\ 0 & 0 & \mu_{33}\end{bmatrix}\begin{bmatrix}\frac{\partial}{\partial x}\tilde{\Phi}(x,y,z,t)\\ \frac{\partial}{\partial y}\tilde{\Phi}(x,y,z,t)\\ \frac{\partial}{\partial z}\tilde{\Phi}(x,y,z,t)\end{bmatrix}, \tag{10}$$

Where, Q, r, k_f and $\widetilde{\Phi}$ represent elastic constant, piezomagnetic constant, shear correction factor (which is equal to 5/6) and magnetic potential field. The magnetic potential field assumes to be: $\widetilde{\Phi}(x,y,z,t) = -\Phi(x,y,t)\cos\left(\frac{\pi z}{h_c}\right)$. (Ebrahimi *et al*. 2019b)

Also, B and μ denote magnetic induction and magnetic permeability coefficient, respectively. Finally, Using Eqs. (1-10), the kinetic and strain energy of Piezomagnetic core have derived as (Ke *et al*. 2010)

$$K^c = \int_V \frac{1}{2}\rho_c \begin{bmatrix} \left(\frac{\partial}{\partial t}\tilde{u}(x,y,z,t)\right)^2 + \\ +\left(\frac{\partial}{\partial t}\tilde{v}(x,y,z,t)\right)^2 \\ +\left(\frac{\partial}{\partial t}\tilde{w}(x,y,z,t)\right)^2 \end{bmatrix} d\forall, \tag{11}$$

$$\begin{aligned} \cup^c = \int_v \frac{1}{2}\big[&\sigma_{xx}^c\varepsilon_{xx}^c + \sigma_{yy}^c\varepsilon_{yy}^c + 2\sigma_{xy}^c\varepsilon_{xy}^c + 2\sigma_{xz}^c\varepsilon_{xz}^c \\ &+2\sigma_{yz}^c\varepsilon_{yz}^c + \Big\{B_x\frac{\partial}{\partial x}\widetilde{\Phi}(x,y,z,t) \\ &+B_y\frac{\partial}{\partial y}\widetilde{\Phi}(x,y,z,t) + B_z\frac{\partial}{\partial z}\widetilde{\Phi}(x,y,z,t)\Big\}\big] d\forall, \end{aligned} \tag{12}$$

2.2 Flexoelectric face sheets

The linear form of piezoelectricity theory has hired to show the effect of flexoelectricity. The higher order terms are neglected to simplify the equations (Robinson *et al*. 2012, Zhang and Jiang 2014, Zubko *et al*. 2013). So, the internal energy density for flexoelectric face sheets can be defined as Zhang and Jiang (2014)

$$\begin{aligned} \cup = &\frac{1}{2}a_{kl}P_kP_l + \frac{1}{2}c_{ijkl}\varepsilon_{ij}\varepsilon_{kl} + d_{ijk}\varepsilon_{ij}P_k \\ &+\frac{1}{2}b_{ijkl}P_{i,j}P_{k,l} + f_{ijkl}u_{i,jk}P_l + e_{ijkl}\varepsilon_{ij}P_{k,l}, \end{aligned} \tag{13}$$

where P_i, ε_{ij}, a_{kl}, c_{ijkl} and d_{ijk} are, respectively, polarization, strain, dielectric, elastic and piezoelectric constant tensors. The polarization gradient and polarization gradient coupling tensor represents by b_{ijkl}. f_{ijkl} is the strain gradient and polarization coupling tensor. e_{ijkl} denotes the strain and polarization gradient coupling and $f_{ijkl} = -e_{ijkl}$ (Sharma *et al*. 2010, Shen and Hu 2010). Consequently, the constitutive equations for flexoelectric face sheets can be derived as Hu and Shen (2010)

$$\sigma_{ij} = \frac{\partial \cup}{\partial \varepsilon_{ij}} = c_{ijkl}\varepsilon_{kl} + d_{ijk}P_k + e_{ijkl}P_{k,l}, \tag{14}$$

$$\sigma_{ijm} = \frac{\partial \cup}{\partial u_{i,jm}} = f_{ijmk}P_k, \tag{15}$$

$$E_i = \frac{\partial \cup}{\partial P_i} = a_{ij}P_j + d_{jki}\varepsilon_{jk} + f_{jkli}u_{j,kl}, \tag{16}$$

$$E_{ij} = \frac{\partial \cup}{\partial P_{i,j}} = b_{ijkl}P_{k,l} + e_{klij}\varepsilon_{kl}, \tag{17}$$

where σ_{ij}, E_i, σ_{ijm} and E_{ij} represent stress, electrical field, higher order stress and higher order electrical field tensors, respectively. Moreover, the strain equations can be represented as follows Ansari and Sahmani (2011)

$$\begin{aligned} &\varepsilon_{xx} = \frac{\partial\tilde{u}}{\partial x}, && \varepsilon_{yy} = \frac{\partial\tilde{v}}{\partial y}, \\ &\varepsilon_{xy} = \frac{1}{2}\left(\frac{\partial\tilde{v}}{\partial x} + \frac{\partial\tilde{u}}{\partial y}\right), && \gamma_{xxz} = \frac{\partial\varepsilon_{xx}}{\partial z}, \\ &\gamma_{yyz} = \frac{\partial\varepsilon_{yy}}{\partial z}, && \gamma_{xyz} = \frac{\partial(2\varepsilon_{xy})}{\partial z}, \\ &\gamma_{xz} = 0, && \gamma_{yz} = 0 \end{aligned} \tag{18}$$

Some assumptions are needed to mention the equations in a simple form as: $c_{11} = c_{1111}$, $c_{66} = c_{1212}$, $d_{31} = d_{311}$, $a_{33} = a_{3333}$, and $b_{33} = b_{3333}$, $f_{1133} = f_{2233} = f_{19}$ (Shu *et al*. 2011). According to Fig. 1, the electric field E_i only exists in the z direction {Formatting Citation} and using Eqs. (16)-(18), the higher order electric field E_{ij} for flexoelectric face sheets can be derived as

$$E_z = a_{33}P_z + d_{31}(\varepsilon_{xx} + \varepsilon_{yy}) + f_{19}\left(\frac{\partial\varepsilon_{xx}}{\partial z} + \frac{\partial\varepsilon_{yy}}{\partial z}\right), \tag{19}$$

$$E_{zx} = b_{3133}P_{z,z}, \tag{20}$$

$$E_{zy} = b_{3233}P_{z,z}, \tag{21}$$

$$E_{zz} = b_{33}P_{z,z} - f_{19}(\varepsilon_{xx} + \varepsilon_{yy}). \tag{22}$$

When the flexoelectric face sheet is under an electric potential φ across z direction (across its thickness), the equilibrium equation should be satisfied as (Hu and Shen 2010, Shen and Hu 2010)

$$E_z + \frac{\partial\varphi}{\partial z} - E_{zx,x} - E_{zy,y} - E_{zz,z} = 0, \tag{23}$$

where φ is the electric potential along with z axis. When there is not any free electric charge on the flexoelectric face sheet, the Gauss's law can be written as Hu and Shen (2010)

$$-k\varphi_{,zz} + P_{z,z} = 0, \tag{24}$$

where $k = k_0k_b$, $k_0 = 8.85\times10^{-12}CV^{-1}m^{-1}$ is the permittivity of the air and $k_b = 6.62$ is the background permittivity of $BaTiO_3$ when its electric field is across the polarization direction Tagantsev and Gerra (2006). Using Eqs. (19)-(24) and the electric boundary conditions $E_{ij}n_j = 0$, $\varphi_{\left(\frac{h}{2}\right)} = V_0$ and $\varphi_{\left(-\frac{h}{2}\right)} = 0$ for flexoelectric face sheets, the electric potential can be derived in terms of transverse displacement, rotations of middle surface and applied voltage V_0 as

$$\varphi(x,y,z,t)=\frac{d_{31}\left(z^2-\frac{h^2}{4}\right)\left(\frac{\partial^2 w}{\partial x^2}+\frac{\partial^2 w}{\partial y^2}\right)}{2(a_{33}k+1)}+\frac{V_0}{h}z+\frac{V_0}{2}+\frac{f_{19}z\left(\frac{\partial^2 w}{\partial x^2}+\frac{\partial^2 w}{\partial y^2}\right)}{(a_{33}k+1)}$$
$$-\frac{f_{19}h\left(e^{\lambda_2 z}-\left(e^{\lambda_2 z}\right)^{-1}\right)\left(\frac{\partial^2 w}{\partial x^2}+\frac{\partial^2 w}{\partial y^2}\right)\left(e^{\frac{\lambda_2 h}{2}}-\left(e^{\frac{\lambda_2 h}{2}}\right)^{-1}\right)^{-1}}{2(a_{33}k+1)} \tag{25}$$
$$+\frac{b_{33}kd_{31}}{(a_{33}k+1)^2}\left(1-\frac{e^{\lambda_2 z}+\left(e^{\lambda_2 z}\right)^{-1}}{e^{\frac{\lambda_2 h}{2}}+\left(e^{\frac{\lambda_2 h}{2}}\right)^{-1}}\right)+\left(\frac{\partial^2 w}{\partial x^2}+\frac{\partial^2 w}{\partial y^2}\right)-\frac{f_{19}}{(a_{33}k+1)}\left(1-\frac{e^{\lambda_2 z}+\left(e^{\lambda_2 z}\right)^{-1}}{e^{\frac{\lambda_2 h}{2}}+\left(e^{\frac{\lambda_2 h}{2}}\right)^{-1}}\right)\left(\frac{\partial u}{\partial x}+\frac{\partial v}{\partial y}\right),$$

where $\lambda_2=\sqrt{\frac{1+ka_{33}}{kb_{33}}}$.

Using Eqs. (23)-(24) the polarization is

$$P_z=2\frac{kd_{31}z\left(\frac{\partial^2 w}{\partial x^2}+\frac{\partial^2 w}{\partial y^2}\right)}{2(a_{33}k+1)}+\frac{kV_0}{h}+\frac{kf_{19}\left(\frac{\partial^2 w}{\partial x^2}+\frac{\partial^2 w}{\partial y^2}\right)}{(a_{33}k+1)}-\frac{b_{33}k^2d_{31}\left(e^{\lambda_2 z}\lambda_2-\frac{\lambda_2}{e^{\lambda_2 z}}\right)\left(\frac{\partial^2 w}{\partial x^2}+\frac{\partial^2 w}{\partial y^2}\right)\left(e^{\frac{\lambda_2 h}{2}}+\left(e^{\frac{\lambda_2 h}{2}}\right)^{-1}\right)^{-1}}{(a_{33}k+1)^2}$$
$$-\frac{kf_{19}h\left(e^{\lambda_2 z}\lambda_2+\frac{\lambda_2}{e^{\lambda_2 z}}\right)\left(\frac{\partial^2 w}{\partial x^2}+\frac{\partial^2 w}{\partial y^2}\right)\left(e^{\frac{\lambda_2 h}{2}}-\left(e^{\frac{\lambda_2 h}{2}}\right)^{-1}\right)^{-1}}{2(a_{33}k+1)}+\frac{kf_{19}\left(e^{\lambda_2 z}\lambda_2-\frac{\lambda_2}{e^{\lambda_2 z}}\right)\left(\frac{\partial u}{\partial x}+\frac{\partial v}{\partial y}\right)\left(e^{\frac{\lambda_2 h}{2}}+\left(e^{\frac{\lambda_2 h}{2}}\right)^{-1}\right)^{-1}}{(a_{33}k+1)}. \tag{26}$$

Substitution of Eq. (26) into Eqs. (19) and (22), respectively, electrical field in the z direction (E_z) and the higher order electric field (E_{zz}) for top and bottom flexoelectric face sheets can be obtained as

$$E_z=a_{33}k\left(2\frac{d_{31}z\left(+\frac{\partial^2 w}{\partial x^2}+\frac{\partial^2 w}{\partial y^2}\right)}{2(a_{33}k+1)}+\frac{V_0}{h}+\frac{f_{19}\left(+\frac{\partial^2 w}{\partial x^2}+\frac{\partial^2 w}{\partial y^2}\right)}{(a_{33}k+1)}-\frac{f_{19}h}{2(a_{33}k+1)}\left(e^{\lambda_2 z}\lambda_2+\frac{\lambda_2}{e^{\lambda_2 z}}\right)\left(+\frac{\partial^2 w}{\partial x^2}+\frac{\partial^2 w}{\partial y^2}\right)\left(e^{\frac{\lambda_2 h}{2}}-\left(e^{\frac{\lambda_2 h}{2}}\right)^{-1}\right)^{-1}\right.$$
$$-\frac{b_{33}kd_{31}}{(a_{33}k+1)^2}\left(e^{\lambda_2 z}\lambda_2-\frac{\lambda_2}{e^{\lambda_2 z}}\right)\left(+\frac{\partial^2 w}{\partial x^2}+\frac{\partial^2 w}{\partial y^2}\right)\left(e^{\frac{\lambda_2 h}{2}}+\left(e^{\frac{\lambda_2 h}{2}}\right)^{-1}\right)^{-1} \tag{27}$$
$$\left.+\frac{f_{19}}{(a_{33}k+1)}\left(e^{\lambda_2 z}\lambda_2-\frac{\lambda_2}{e^{\lambda_2 z}}\right)\left(\frac{\partial u}{\partial x}+\frac{\partial v}{\partial y}\right)\left(e^{\frac{\lambda_2 h}{2}}+\left(e^{\frac{\lambda_2 h}{2}}\right)^{-1}\right)^{-1}\right)+d_{31}\left(\frac{\partial u}{\partial x}+\frac{\partial v}{\partial y}-z\frac{\partial^2 w}{\partial x^2}-z\frac{\partial^2 w}{\partial y^2}\right)+k_s f_{19}\left(-\frac{\partial^2 w}{\partial x^2}-\frac{\partial^2 w}{\partial y^2}\right),$$

$$E_{zz}=b_{33}k\left(\frac{d_{31}\left(\frac{\partial^2 w}{\partial x^2}+\frac{\partial^2 w}{\partial y^2}\right)}{(a_{33}k+1)}-\frac{f_{19}h}{(a_{33}k+1)}\left(e^{\lambda_2 z}{\lambda_2}^2-\frac{{\lambda_2}^2}{e^{\lambda_2 z}}\right)\left(\frac{\partial^2 w}{\partial x^2}+\frac{\partial^2 w}{\partial y^2}\right)\left(e^{\frac{\lambda_2 h}{2}}-\left(e^{\frac{\lambda_2 h}{2}}\right)^{-1}\right)^{-1}\right.$$
$$-\frac{b_{33}kd_{31}}{(a_{33}k+1)^2}\left(2e^{\lambda_2 z}{\lambda_2}^2+\frac{2{\lambda_2}^2}{e^{\lambda_2 z}}\right)\left(\frac{\partial^2 w}{\partial x^2}+\frac{\partial^2 w}{\partial y^2}\right)\left(e^{\frac{\lambda_2 h}{2}}+\left(e^{\frac{\lambda_2 h}{2}}\right)^{-1}\right)^{-1} \tag{28}$$
$$\left.+\frac{f_{19}}{(a_{33}k+1)}\left(2e^{\lambda_2 z}{\lambda_2}^2+\frac{2{\lambda_2}^2}{e^{\lambda_2 z}}\right)\left(\frac{\partial u}{\partial x}+\frac{\partial v}{\partial y}\right)\left(e^{\frac{\lambda_2 h}{2}}+\left(e^{\frac{\lambda_2 h}{2}}\right)^{-1}\right)^{-1}\right)-f_{19}\left(\frac{\partial u}{\partial x}-z\frac{\partial^2 w}{\partial x^2}+\frac{\partial v}{\partial y}-z\frac{\partial^2 w}{\partial y^2}\right).$$

After the derivation of electric field terms, the stresses of flexoelectric face sheets can be determined from the constitutive as follows

$$\begin{Bmatrix}\sigma_{xx}\\ \sigma_{yy}\\ \sigma_{xy}\\ \tau_{xxz}\\ \tau_{yyz}\\ \tau_{xyz}\end{Bmatrix}=\begin{bmatrix}c_{11}&c_{12}&0&0&0&0\\ c_{21}&c_{22}&0&0&0&0\\ 0&0&c_{66}&0&0&0\\ 0&0&0&0&0&0\\ 0&0&0&0&0&0\\ 0&0&0&0&0&0\end{bmatrix}\begin{Bmatrix}\varepsilon_{xx}\\ \varepsilon_{yy}\\ 2\varepsilon_{xy}\\ \gamma_{xxz}\\ \gamma_{yyz}\\ \gamma_{xyz}\end{Bmatrix}$$
$$+\begin{bmatrix}d_{31}k&k_s f_{19}k\\ d_{32}k&k_s f_{19}k\\ 0&0\\ k_s f_{19}k&0\\ k_s f_{19}k&0\\ 0&0\end{bmatrix}\begin{Bmatrix}\frac{\partial\varphi}{\partial z}\\ -\frac{\partial^2\varphi}{\partial z^2}\end{Bmatrix}, \tag{29}$$

in Eq. (29), k_s is shear correction factor which is equal to 5/6.

At the end, using Eqs. (1)-(3), (18), (25)-(28) and (29), the kinetic and strain energy of flexoelectric face sheets can be defined as Liu *et al*. (2012)

$$K^f=\int_V\frac{1}{2}\rho_f\begin{bmatrix}\left(\frac{\partial}{\partial t}\tilde{u}(x,y,z,t)\right)^2\\ +\left(\frac{\partial}{\partial t}\tilde{v}(x,y,z,t)\right)^2\\ +\left(\frac{\partial}{\partial t}\tilde{w}(x,y,z,t)\right)^2\end{bmatrix}d\forall, \tag{30}$$

$$\cup^f = \int_v \frac{1}{2}\Big(\sigma_{xx}\varepsilon_{xx} + \sigma_{yy}\varepsilon_{yy} + 2\sigma_{xy}\varepsilon_{xy} + \tau_{xxz}\gamma_{xxz} + \tau_{yyz}\gamma_{yyz} + \tau_{xyz}\gamma_{xyz} + E_z p_z + E_{zz}\frac{\partial}{\partial z}p_z - k\left(\frac{\partial}{\partial z}\varphi(x,y,z,t)\right)^2 + p_z\frac{\partial}{\partial z}\varphi(x,y,z,t)\Big)d\forall, \quad (31)$$

2.3 Modified couple stress theory (MCST)

According to statistics and different researches, it has revealed that Modified Couple Stress Theory is more accurate than Nonlocal theory. So, the MCST has utilized to consider the size effect of the aforementioned sandwich plate. So, the strain equations can be obtained as

$$\varepsilon_{xx}{}^m = \frac{\partial \tilde{u}}{\partial x}, \quad \varepsilon_{yy}{}^m = \frac{\partial \tilde{v}}{\partial y}, \quad \varepsilon_{xy}{}^m = \frac{1}{2}\left(\frac{\partial \tilde{u}}{\partial y} + \frac{\partial \tilde{v}}{\partial x}\right)$$
$$\varepsilon_{xz}{}^m = \frac{1}{2}\left(\frac{\partial \tilde{u}}{\partial z} + \frac{\partial \tilde{w}}{\partial x}\right), \quad \varepsilon_{yz}{}^m = \frac{1}{2}\left(\frac{\partial \tilde{v}}{\partial z} + \frac{\partial \tilde{w}}{\partial y}\right), \quad (32)$$

Which the superscript m denotes MCST. The stress tensor can be defined as Yang *et al*. (2011)

$$\begin{bmatrix}\sigma_{xx}{}^m\\ \sigma_{yy}{}^m\\ \sigma_{xy}{}^m\\ \sigma_{yz}{}^m\\ \sigma_{xz}{}^m\end{bmatrix} = \begin{bmatrix}Q_{11} & Q_{12} & 0 & 0 & 0\\ Q_{12} & Q_{22} & 0 & 0 & 0\\ 0 & 0 & Q_{66} & 0 & 0\\ 0 & 0 & 0 & k_f Q_{44} & 0\\ 0 & 0 & 0 & 0 & k_f Q_{55}\end{bmatrix}\begin{bmatrix}\varepsilon_{xx}{}^m\\ \varepsilon_{yy}{}^m\\ 2\varepsilon_{xy}{}^m\\ 2\varepsilon_{yz}{}^m\\ 2\varepsilon_{xz}{}^m\end{bmatrix}. \quad (33)$$

The equation of strain energy is presented as follows Rahmani *et al*. (2018)

$$\cup^m = \int_V \frac{1}{2}\begin{bmatrix}\sigma_{xx}{}^m\varepsilon_{xx}{}^m + \sigma_{yy}{}^m\varepsilon_{yy}{}^m \\ +2\sigma_{xy}{}^m\varepsilon_{xy}{}^m + 2\sigma_{xz}{}^m\varepsilon_{xz}{}^m \\ +2\sigma_{yz}{}^m\varepsilon_{yz}{}^m \\ + \begin{Bmatrix} m_{xx}\chi_{xx} + m_{yy}\chi_{yy} \\ +m_{xy}\chi_{xy} + m_{xz}\chi_{xz} \\ +m_{yz}\chi_{yz}\end{Bmatrix}\end{bmatrix} d\forall, \quad (34)$$

Where, m_{lk} and χ_{lk} are stress and symmetric curvature tensor. As another expression, m_{lk} is a part of couple stress tensor which is ignorable in macro-scale whereas, plays a crucial role in micro and nano-scale.

m_{lk} and χ_{lk} can be presented as

$$\chi_{xx} = \frac{\partial^2 w}{\partial y \partial x}, \quad \chi_{yy} = -\frac{\partial^2 w}{\partial y \partial x}$$
$$\chi_{xy} = \frac{1}{2}\left(\frac{\partial^2 w}{\partial y^2} - \frac{\partial^2 w}{\partial x^2}\right), \quad \chi_{xz} = \frac{1}{4}\left(\frac{\partial^2 v}{\partial x^2} - \frac{\partial^2 u}{\partial y \partial x}\right) \quad (35)$$
$$\chi_{yz} = \frac{1}{4}\left(\frac{\partial^2 v}{\partial y \partial x} - \frac{\partial^2 u}{\partial y^2}\right), \quad \chi_{zz} = 0$$

$$m_{lk} = 2{l_0}^2 G\chi_{lk}, \quad (36)$$

Where, l_0 is material length scale parameter and G assumes to be equal to Q_{66}.

Substituting Eqs. (33)-(36) to Eq. (34), the strain energy due to MCST can be obtained.

3. Governing equations

Hamilton's principle has used to extract the governing equations as follows (Arshid and Khorshidvand 2018, Guerroudj *et al*. 2018, Ebrahimi *et al*. 2017)

$$\delta\Pi = \delta\int_{t_1}^{t_2}\left((\cup^c - K^c) + (\cup^f - K^f) + \cup^m - \Sigma\right)dt = 0, \quad (37)$$

in which, $\cup$, K and Σ represent strain energy, kinetic energy and external work, respectively. Superscripts c, f and m are, respectively, representative of the words, core, face sheets and MCST.

Visco-Pasternak foundation is capable to consider normal and transverse shear loads. The force applied on sandwich plate due to Visco-Pasternak foundation can be determined as (Arshid *et al*. 2019, Yazid *et al*. 2018, Zenkour 2015, Anh *et al*. 2015)

$$F^{Visco-Pasternak foundation} = K_w w(x,y,t) - K_{gx}\frac{\partial^2 w(x,y,t)}{\partial x^2} - K_{gy}\frac{\partial^2 w(x,y,t)}{\partial y^2} + C_d\frac{\partial^2 w(x,y,t)}{\partial t}, \quad (38)$$

where K_w is Winkler spring coefficient and K_{gx}, K_{gy} are shear layer parameters in x and y directions, respectively. Also, C_d is damping constant. Therefore, the work of elastic medium is as follows

$$\Sigma = \frac{1}{2}\int_A F^{Visco-Pasternak foundation} w dA, \quad (39)$$

Substitution of Eqs. (11)-(12), (30)-(31), (34) and (39) into Eq. (37), the equations of motion can be obtained by setting the coefficientsδu, δv, $\delta\Phi$ and δw equal to zero.

4. Analytical solution procedure

In the case of considering different boundary conditions and in order to separate variables related to space and time for sandwich plate, the displacement components can be defined as Wattanasakulpong and Chaikittiratana (2015)

$$\begin{aligned} u(x,y,t) &= \sum_{m=1}^{M}\sum_{n=1}^{N} U_{mn}\frac{dX_m(x)}{dx}Y_n(y)e^{i\omega_{mn}t}, v(x,y,t) \\ &= \sum_{m=1}^{M}\sum_{n=1}^{N} V_{mn}\frac{dY_n(y)}{dy}X_m(x)e^{i\omega_{mn}t}, w(x,y,t) \\ &= \sum_{m=1}^{M}\sum_{n=1}^{N} W_{mn}X_m(x)Y_n(y)e^{i\omega_{mn}t}, \Phi(x,y,t) \\ &= \sum_{m=1}^{M}\sum_{n=1}^{N} \Phi_{mn}X_m(x)Y_n(y)e^{i\omega_{mn}t}, \end{aligned} \quad (40)$$

in which $X(x)$ and $Y(y)$ are hired to switch among different boundary conditions and define as follow

$$X_m(x) = sin(\varpi_m x) + \zeta_m cos(\varpi_m x) + \eta_m sinh(\varpi_m x) + \xi_m cosh(\varpi_m x), \quad (41)$$

Table 1 Different boundary condition constants

B.c.	SSSS	SSCS	CCCC
ϖ_m	$\frac{m\pi}{a}$	$\frac{m\pi}{a}$	$\frac{(2m+1)\pi}{2a}$
ϖ_n	$\frac{n\pi}{b}$	$\frac{(4n+1)\pi}{4b}$	$\frac{(2n+1)\pi}{2b}$
ζ_m	0	0	$\frac{-(sin(\varpi_m a)-sinh(\varpi_m a)}{cos(\varpi_m a)-cosh(\varpi_m a)}$
ζ_n	0	0	$\frac{-(sin(\varpi_n b)-sinh(\varpi_n b))}{cos(\varpi_n b)-cosh(\varpi_n b)}$
η_m	0	0	-1
η_n	0	$\frac{-\sin\varpi_n b}{sinh\,\varpi_n b}$	-1
ξ_m	0	0	$-\zeta_m$
ξ_n	0	0	$-\zeta_n$
ϖ_m	$\frac{(4m+1)\pi}{4a}$	$\frac{(2m-1)\pi}{4a}$	$\frac{(2m-1)\pi}{4a}$
ϖ_n	$\frac{(4n+1)\pi}{4b}$	$\frac{(2n-1)\pi}{4b}$	$\frac{(4n+1)\pi}{4b}$
ζ_m	0	$\frac{-(sin(\varpi_m a)+sinh(\varpi_m a)}{cos(\varpi_m a)+cosh(\varpi_m a)}$	$\frac{-(sin(\varpi_m a)+sinh(\varpi_m a)}{cos(\varpi_m a)+cosh(\varpi_m a)}$
ζ_n	0	$\frac{-(sin(\varpi_n b)+sinh(\varpi_n b))}{cos(\varpi_n b)+cosh(\varpi_n b)}$	0
η_m	$\frac{-\sin\varpi_m a}{sinh\,\varpi_m a}$	-1	-1
η_n	$\frac{-\sin\varpi_n b}{sinh\,\varpi_n b}$	-1	$\frac{-\sin\varpi_n b}{sinh\,\varpi_n b}$
ξ_m	0	$-\zeta_m$	$-\zeta_m$
ξ_n	0	$-\zeta_n$	0
ϖ_m	$\frac{(4m+1)\pi}{4a}$	$\frac{(2m-1)\pi}{4a}$	$\frac{(2m-1)\pi}{4a}$
ϖ_n	$\frac{(4n+1)\pi}{4b}$	$\frac{(2n-1)\pi}{4b}$	$\frac{(4n+1)\pi}{4b}$

$$Y_n(x) = sin(\varpi_n y) + \zeta_n\, cos(\varpi_n y) + \eta_n\, sinh(\varpi_n y) + \xi_n\, cosh(\varpi_n y). \quad (41)$$

All constants related to these equations for different boundary conditions are listed in Table 1 as below.

U_{mn}, V_{mn}, W_{mn} and Φ_{mn} are unknown coefficients of each mode and ω_{mn} represents the natural frequency. The mode numbers along x and y directions are, respectively, m and n. Eventually, the equations of motion can be defined as a matric form as

$$\begin{bmatrix} T_{11} & T_{12} & T_{13} & T_{14} \\ T_{21} & T_{22} & T_{23} & T_{24} \\ T_{31} & T_{32} & T_{33} & T_{34} \\ T_{41} & T_{42} & T_{43} & T_{44} \end{bmatrix} \begin{bmatrix} U_{mn} \\ V_{mn} \\ W_{mn} \\ \Phi_{mn} \end{bmatrix} = \begin{bmatrix} 0 \\ 0 \\ 0 \\ 0 \end{bmatrix}. \quad (42)$$

The arrays of matric [T] are obtained by substituting Eq. (40) into the governing equation of motion which have obtained in previous section.

5. Numerical results and discussions

In this section, numerical and graphical results have collected to investigate the effect of flexoelectricity on vibrational behavior of sandwich plate with piezomagnetic core made by $CoFe_2O_4$, and $BaTiO_3$ as flexoelectric face sheets. The material properties of $CoFe_2O_4$ are expressed in Table 2 (Ebrahimi and Barati 2016). Also, the properties for $BaTiO_3$ as flexoelectric face sheets are indicated in Table 3. (Zhang and Jiang 2014, Zhang *et al*. 2014)

The geometrical and mechanical properties of sandwich plate are considered as follows

$$h_c = 2(nm), \quad h_f = 0.1(nm), \quad a = 20h, \quad \frac{a}{b} = 1, \quad K_w = 10^9(N/m^3), \quad K_{gx} = 100(N/m), \quad K^* = \frac{K_{gy}}{K_{gx}}, \quad C_d = 10^{18}(Kg/s).$$

In order to guaranty the reliability of the results of this research, the effects of aspect ratio (a/b) and thickness to length ratio (h/a) on the non-dimensional fundamental

Table 2 The Mechanical properties of Piezomagnetic layer ($CoFe_2O_4$) (Ebrahimi and Barati 2016)

$\rho_c(kg/m^3)$	$Q_{11}(GPa)$	$Q_{12}(GPa)$	$Q_{22}(GPa)$	$Q_{44}(GPa)$
5300	286	173	286	45.3
$Q_{55}(GPa)$	$Q_{66}(GPa)$	$r_{31}(N/Am)$	$\mu_{11}=\mu_{22}(Ns^2/C^2)$	$\mu_{33}(Ns^2/C^2)$
45.3	56.5	580.3	$-590e-6$	$157e-6$

Table 3 The mechanical properties of flexoelectric face sheets ($BaTiO_3$) (Zhang and Jiang 2014, Zhang *et al*. 2014)

$\rho_f(kg/m^3)$	$c_{11}=c_{22}(GPa)$	$c_{12}=c_{21}(GPa)$	$c_{66}(GPa)$	$\rho_f(kg/m^3)$
6020	167.55	78.15	44.7	6020
$a_{33}(Vm/C)$	$b_{33}(Jm^3/C^2)$	$d_{31}=d_{32}(V/m)$	$f_{19}(V)$	$a_{33}(Vm/C)$
0.79×10^8	1×10^{-9}	3.5×10^8	10	0.79×10^8

Table 4 Comparison among the non-dimensional natural frequency of *SSSS* plates in present study and (Aghababaei and Reddy 2009, Hosseini-Hashemi *et al*. 2015)

a/b	h/a	Author(s)	Theory	Frequency	Error (%)
1.0	0.1	Aghababaei and Reddy (2009)	HSDT	19.1678	2.1
		Hosseini-Hashemi *et al*. (2015)	HSDT	19.0653	2.6
		Present		19.5788	
1.0	0.05	Aghababaei and Reddy (2009)	HSDT	19.6695	0.15
		Hosseini-Hashemi *et al*. (2015)	HSDT	19.5625	0.69
		Present		19.6987	
0.5	0.1	Aghababaei and Reddy (2009)	HSDT	12.1157	1.3
		Hosseini-Hashemi *et al*. (2015)	HSDT	12.0675	1.7
		Present		12.2741	
0.5	0.05	Aghababaei and Reddy (2009)	HSDT	12.3445	0.18
		Hosseini-Hashemi *et al*. (2015)	HSDT	12.2675	0.44
		Present		12.3212	

natural frequency of *SSSS* plates compared with (Aghababaei and Reddy 2009 and Hosseini-Hashemi *et al*. 2015) in Table 4. Moreover, the effect of different mode numbers on the dimensionless natural frequencies of the piezoelectric plate in present study has compared with Liu *et al*. (2013) in Table 5.

Finally, using Tables 4-5, it is clear that a good agreement exists among the results of present study and those of Aghababaei and Reddy (2009), Hosseini-Hashemi *et al*. (2015), Liu *et al*. (2013).

The natural frequency of sandwich plate versus width to thickness ratio (b/h) for different mode number is shown in

Table 5 Comparison of dimensionless natural frequencies of the piezoelectric nanoplate in different mode numbers

Frequency	Liu *et al*. (2013)	Present	Error (%)
ω_{11}	0.6634	0.6902	4
ω_{12}	1.6518	1.6601	0.5
ω_{22}	2.6328	2.6962	2.4
ω_{13}	3.2829	3.2175	1.9

Fig. 2. By increasing (b/h), the natural frequency of sandwich plate decreases. This behavior is due to the flexibility enhancement of sandwich plate which leads to stiffness and stability reduction. It is also found that in higher mode shapes, higher natural frequency observe in each (b/h).

Fig. 3 denotes the damping constant effect on the natural frequency of sandwich plate versus the thickness of piezo-magnetic core. This figure proved when damping constant increases, the stiffness of system decreases. As another expression, the ability of damping and attracting energy in dampers decreases by damping constant enhancement. So, the natural frequency decreases. Moreover, the natural frequency decreases by increasing in the thickness of piezomagnetic core. In fact, the stability and natural frequency of system reduces when the thickness of piezomagnetic core increases.

Fig. 4 indicates the variations of natural frequency versus thickness of flexoelectric face sheets using Modified couple stress theory for different boundary conditions. It is observed that when the thickness of flexoelectric face sheets increases, the flexibility of sandwich plate increases and leads to increase the energy dissipation and natural frequency reduction in system. So, the control of vibrational behavior of sandwich plates is doable with change in thickness of flexoelectric face sheets in each case of boundary condition.

In Fig. 5 based on the present analytical solutions, results have plotted for each of the five possible cases of boundary conditions (i.e., *SSSS*, *SSCS*, *CSCS*, *CCCC* and *FCCS*). *S* and *C* mean simply and clamped supports respectively. Clamped support related to an edge of structure

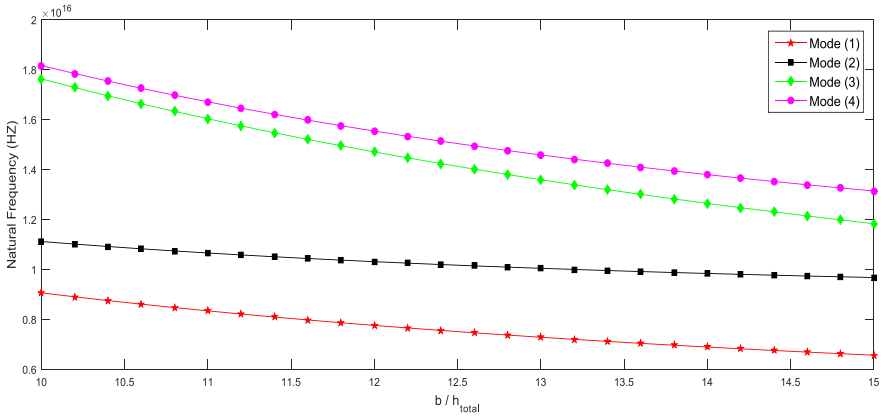

Fig. 2 Variations of Natural frequency versus width to thickness ratio (b/h) for different mode number

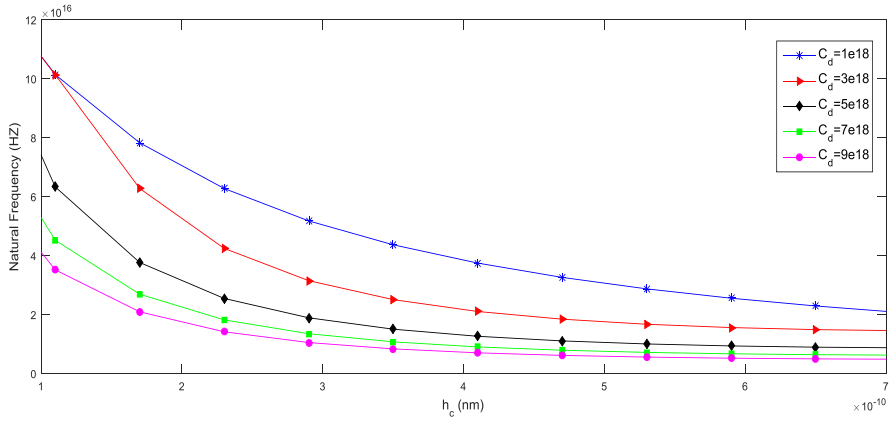

Fig. 3 Variations of Natural frequency versus thickness of piezo magnetic core subjected to different damping coefficients

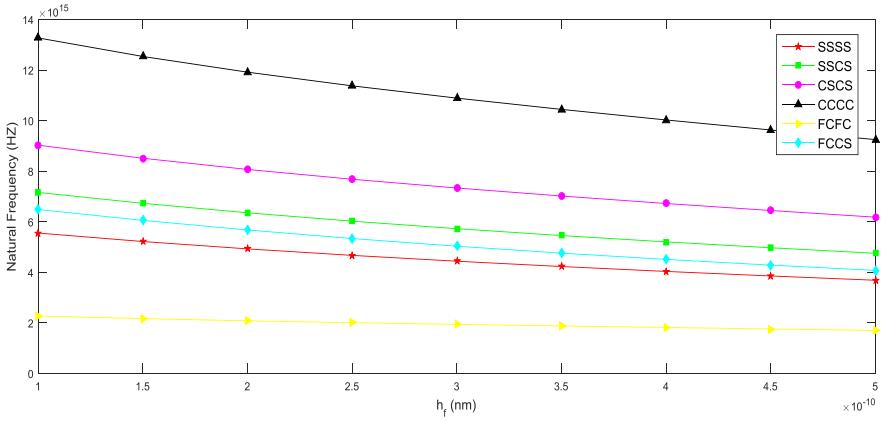

Fig. 4 Variations of natural frequency versus thickness of flexoelectric face sheets and diverse boundary conditions

structure increases the stiffness of system. Stiffness enhancement leads to flexibility reduction and more stable system. So, boundary condition including clamped supports has higher value of natural frequency in each thickness of flexoelectric face sheets. For each case of the boundary conditions, aspect ratio enhancement results lower values of natural frequencies. It is also found that, after a specific aspect ratio (about $a/b = 2.5$) the natural frequency alternation become ignorable and natural frequency tends to be constant.

Pasternak shear constant values at X direction (K_{gx}) and Y direction (K_{gy}) can influence the natural frequency of system. In Fig. 6 the natural frequency with and without Pasternak foundation has investigated. By putting K_{gx} and K_{gy} equal to zero, it is possible to eliminate the Pasternak foundation from the model related to this study. It has declared that the presence of Pasternak foundation, increases the natural frequency and stiffness level of system and by increasing in Pasternak shear constants value, the Pasternak foundation plays more important rule in natural

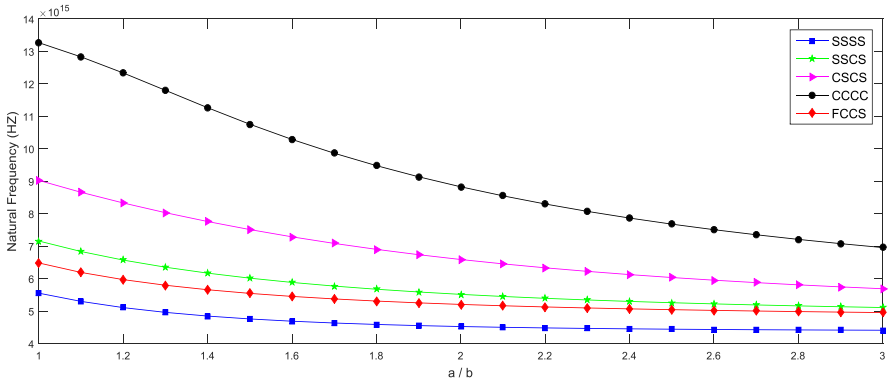

Fig. 5 Variations of natural frequency versus aspect ratio for different boundary conditions

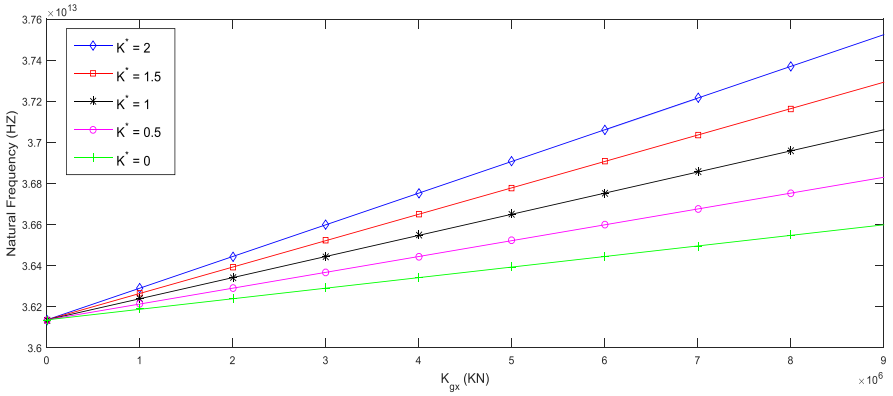

Fig. 6 Variations of natural frequency versus shear layer constant in x direction under different K_{gx} to K_{gy} ratio (K^*)

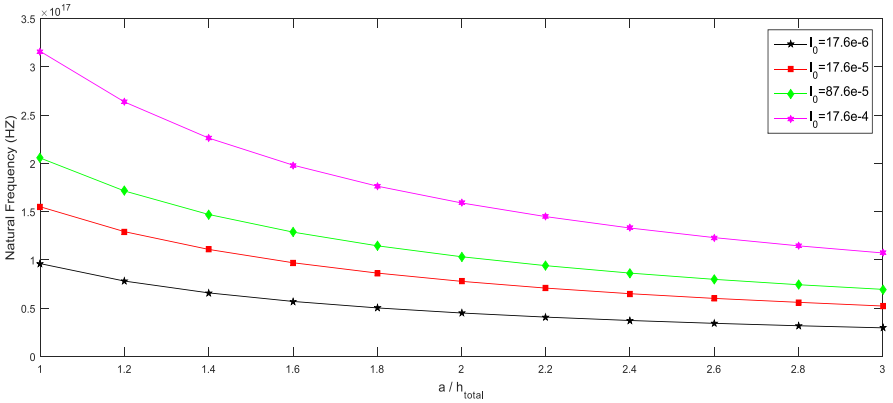

Fig. 7 Variations of natural frequency versus length to thickness ratio (a/h) for different length scale parameter

frequency enlargement. K^* is a constant and can be defined as $K^* = K_{gy}/K_{gx}$. Fig. 6 indicates that in each K_{gx}, the higher values of natural frequency, stiffness and stability of system can be obtained by using higher value of K_{gy} which means using higher value of K^*.

The effect of length scale parameter (l_0) on natural frequency of sandwich plates has investigated in Fig. 7. As it is clear in Eqs. (34), (36)-(37), larger magnitudes of l_0 lead to increase in system strain energy due to the curvature tensor (m_{lk}). Curvature tensor is related to stiffness tensor. Therefore, by length scale parameter enhancement the stiffness and finally natural frequency of system increases.

6. Conclusions

As mentioned in abstract and introduction, flexo-electricity denotes the linear coupling between strain gradient and polarization. Based on previous papers, however flexoelectricity has not a dominant effect in macro scale, its effect plays a crucial role in micro and nano scale. Using Classical plate theory (CPT) and modified couple stress theory (MCST), vibrational behaviour of a sandwich plate with piezomagnetic core and flexoelectric face sheets took into examination in current study. For governing equations elicitation, Hamilton's principle and Navier's

methods have hired. Current research illustrates that thicker layers of flexoelectric face sheets lead to less stiff sandwich plate and consequently, the natural frequency decreases by flexo-face sheet thickness increasing. Moreover, recent paper shows sensitivity of natural frequency to length scale parameter and states natural frequency increases with length scale parameter enhancement. Beside this, it has revealed that boundary conditions act as reducing or increasing parameters for natural frequency. As a physical expression it is worthwhile mentioning that despite of SSSS, by using CCCC as boundary conditions, flexibility of whole system drops down and natural frequency increases. The results in this research demonstrate an excellent agreement with previous works. These results can help to design and manufacturing of smart systems more precisely. The aim of this work is to broad the borders of science related to structures with flexoelectric effects consideration.

References

Aghababaei, R. and Reddy, J.N. (2009), "Nonlocal third-order shear deformation plate theory with application to bending and vibration of plates", *J. Sound Vib.*, **326**(1-2), 277-289. https://doi.org/10.1016/j.jsv.2009.04.044

Anh, V.T.T., Bich, D.H. and Duc, N.D. (2015), "Nonlinear stability analysis of thin FGM annular spherical shells on elastic foundations under external pressure and thermal loads", *Eur. J. Mech. - A/Solids*, **50**, 28-38. https://doi: 10.1016/j.euromechsol.2014.10.004

Ansari, R. and Sahmani, S. (2011), "Surface stress effects on the free vibration behavior of nanoplates", *Int. J. Eng. Sci.*, **49**(11), 1204-1215. https://doi.org/10.1016/j.ijengsci.2011.06.005

Arshid, E. and Khorshidvand, A.R. (2018), "Thin-Walled Structures Free vibration analysis of saturated porous FG circular plates integrated with piezoelectric actuators via differential quadrature method", *Thin Wall. Struct.*, **125**(January), 220-233. https://doi.org/10.1016/j.tws.2018.01.007

Arshid, E., Khorshidvand, A.R. and Khorsandijou, S.M. (2019), "The effect of porosity on free vibration of SPFG circular plates resting on visco-Pasternak elastic foundation based on CPT, FSDT and TSDT", *Struct. Eng. Mech., Int. J.*, **70**(1), 97-112. https://doi.org/10.12989/sem.2019.70.1.097

Barati, M.R. (2017), "Coupled effects of electrical polarization-strain gradient on vibration behavior of double-layered flexoelectric nanoplates", *Smart Struct. Syst., Int. J.*, **20**(5), 573-581. https://doi.org/10.12989/sss.2017.20.5.573

Batou, B., Nebab, M., Bennai, R., Atmane, H.A., Tounsi, A. and Bouremana, M. (2019), "Wave dispersion properties in imperfect sigmoid plates using various HSDTs", *Steel Compos. Struct., Int. J.*, **33**(5), 699-716. https://doi.org/10.12989/scs.2019.33.5.699

Bui, T.Q., Doan, D.H., Van Do, T., Hirose, S. and Duc, N.D. (2016), "High frequency modes meshfree analysis of Reissner–Mindlin plates", *J. Sci. Adv. Mater. Devices*, **1**, 400-412. https://doi: 10.1016/j.jsamd.2016.08.005

Cong, P.H., Chien, T.M., Khoa, N.D. and Duc, N.D. (2018), "Nonlinear thermomechanical buckling and post-buckling response of porous FGM plates using Reddy's HSDT", *Aerosp. Sci. Technol.*, **77**, 419-428. https://doi: 10.1016/j.ast.2018.03.020

Duc, N.D. and Cong, P.H. (2015), "Nonlinear vibration of thick FGM plates on elastic foundation subjected to thermal and mechanical loads using the first-order shear deformation plate theory", *Cogent Eng.*, **2**(1), 1045222. https://doi: 10.1080/23311916.2015.1045222

Duc, N.D. and Quan, T.Q. (2014), "Transient responses of functionally graded double curved shallow shells with temperature-dependent material properties in thermal environment", *Eur. J. Mech. - A/Solids*, **47**, 101-123. https://doi: 10.1016/j.euromechsol.2014.03.002

Duc, N.D. and Thang, P.T. (2014), "Nonlinear buckling of imperfect eccentrically stiffened metal–ceramic–metal S-FGM thin circular cylindrical shells with temperature-dependent properties in thermal environments", *Int. J. Mech. Sci.*, **81**, 17-25. https://doi: 10.1016/j.ijmecsci.2014.01.016

Duc, N.D. and Tung, H.V. (2010), "Mechanical and thermal postbuckling of shear-deformable FGM plates with temperature-dependent properties", *Mech. Compos. Mater.*, **46**, 461-476. https://doi: 10.1007/s11029-010-9163-9

Duc, N.D., Cong, P.H., Anh, V.M., Quang, V.D., Tran, P., Tuan, N.D. and Thinh, N.H. (2015), "Mechanical and thermal stability of eccentrically stiffened functionally graded conical shell panels resting on elastic foundations and in thermal environment", *Compos. Struct.*, **132**, 597-609. https://doi: 10.1016/j.compstruct.2015.05.072

Duc, N.D., Nguyen, P.D. and Khoa, N.D. (2017a), "Nonlinear dynamic analysis and vibration of eccentrically stiffened S-FGM elliptical cylindrical shells surrounded on elastic foundations in thermal environments", *Thin-Wall. Struct.*, **117**, 178-189. https://doi: 10.1016/j.tws.2017.04.013

Duc, N.D., Khoa, N.D. and Thiem, H.T. (2017b), "Nonlinear thermo-mechanical response of eccentrically stiffened Sigmoid FGM circular cylindrical shells subjected to compressive and uniform radial loads using the Reddy's third-order shear deformation shell theory", *Mech. Adv. Mater. Struct.*, **25**, 1156-1167. https://doi: 10.1080/15376494.2017.1341581

Ebrahimi, F. and Barati, M.R. (2016), "An exact solution for buckling analysis of embedded piezo-electro-magnetically actuated nanoscale beams", *Adv. Nano Res., Int. J.*, **4**(2), 65-84. http://doi.org/10.12989/anr.2016.4.2.065

Ebrahimi, F., Daman, M. and Jafari, A. (2017), "Nonlocal strain gradient-based vibration analysis of embedded curved porous piezoelectric nano-beams in thermal environment", *Smart Struct. Syst., Int. J.*, **20**(6), 709-728. https://doi.org/10.12989/sss.2017.20.6.709

Ebrahimi, F., Nouraei, M., Dabbagh, A. and Civalek, O. (2019a), "Buckling analysis of graphene oxide powder-reinforced nanocomposite beams subjected to non-uniform magnetic field", *Struct. Eng. Mech., Int. J.*, **71**(5), 351-361. https://doi.org/10.12989/sem.2019.71.4.351

Ebrahimi, F., Karimiasl, M. and Mahesh, V. (2019b), "Vibration analysis of magneto-flexo-electrically actuated porous rotary nanobeams considering thermal effects via nonlocal strain gradient elasticity theory", *Adv. Nano Res., Int. J.*, **7**(4), 223-231. https://doi.org/10.12989/anr.2019.7.4.223

Fu, J.Y., Zhu, W., Li, N. and Cross, L.E. (2006), "Experimental studies of the converse flexoelectric effect induced by inhomogeneous electric field in a barium strontium titanate composition", *J. Appl. Phys.*, **100**(2), 024112. https://doi.org/10.1063/1.2219990

Guerroudj, H.Z., Yeghnem, R., Kaci, A., Zaoui, F.Z., Benyoucef, S. and Tounsi, A. (2018), "Eigenfrequencies of advanced composite plates using an efficient hybrid quasi-3D shear deformation theory", *Smart Struct. Syst., Int. J.*, **22**(1), 121-132. https://doi.org/10.12989/sss.2018.22.1.121

Hosseini-Hashemi, S., Kermajani, M. and Nazemnezhad, R. (2015), "An analytical study on the buckling and free vibration of rectangular nanoplates using nonlocal third-order shear deformation plate theory", *Eur. J. Mech., A/Solids*, **51**, 29-43. https://doi.org/10.1016/j.euromechsol.2014.11.005

Hu, S. and Shen, S. (2010), "Variational principles and governing equations in nano-dielectrics with the flexoelectric effect", *Sci. China Phys. Mech. Astron.*, **53**(8), 1497-1504.

https://doi.org/10.1007/s11433-010-4039-5
Ke, L.L., Yang, J. and Kitipornchai, S. (2010), "Nonlinear free vibration of functionally graded carbon nanotube-reinforced composite beams", *Compos. Struct.*, **92**(3), 676-683. https://doi.org/10.1016/j.compstruct.2009.09.024
Khoa, N.D., Thiem, H.T. and Duc, N.D. (2017), "Nonlinear buckling and postbuckling of imperfect piezoelectric S-FGM circular cylindrical shells with metal–ceramic–metal layers in thermal environment using Reddy's third-order shear deformation shell theory", *Mech. Adv. Mater. Struct.*, **26**, 248-259. https://doi: 10.1080/15376494.2017.1341583
Kiran, M.C. and Kattimani, S.C. (2018), "Free vibration and static analysis of functionally graded skew magneto-electro-elastic plate", *Smart Struct. Syst., Int. J.*, **21**(4), 493-519. https://doi.org/10.12989/sss.2018.21.4.493
Lao, C.S., Kuang, Q., Wang, Z.L., Park, M.C. and Deng, Y. (2007), "Polymer functionalized piezoelectric-FET as humidity/chemical nanosensors", *Appl. Phys. Lett.*, **90**(26), 2-4. https://doi.org/10.1063/1.2748097
Liu, C., Hu, S. and Shen, S. (2012), "Effect of flexoelectricity on electrostatic potential in a bent piezoelectric nanowire", *Smart Mater. Struct.*, **21**(11), 115024. https://doi.org/10.1088/0964-1726/21/11/115024
Liu, C., Ke, L.L., Wang, Y.S., Yang, J. and Kitipornchai, S. (2013), "Thermo-electro-mechanical vibration of piezoelectric nanoplates based on the nonlocal theory", *Compos. Struct.*, **106**, 167-174. https://doi.org/10.1016/j.compstruct.2013.05.031
Ma, W. and Cross, L.E. (2001), "Observation of the flexoelectric effect in relaxor $Pb(Mg_{1/3}Nb_{2/3})O_3$ ceramics", *Appl. Phys. Lett.*, **78**(19), 2920-2921. https://doi.org/10.1063/1.1356444
Ma, W. and Cross, L.E. (2002), "Flexoelectric polarization of barium strontium titanate in the paraelectric state", *Appl. Phys. Lett.*, **81**(18), 3440-3442. https://doi.org/10.1063/1.1518559
Ma, W. and Cross, L.E. (2006), "Flexoelectricity of barium titanate", *Appl. Phys. Lett.*, **88**(23), 2004-2007. https://doi.org/10.1063/1.2211309
Mahesh, V., Kattimani, S., Harursampath, D. and Trung, N.T. (2019), "Coupled evaluation of the free vibration characteristics of magneto-electro-elastic skew plates in hygrothermal environment", *Smart Struct. Syst., Int. J.*, **24**(2), 267-292. https://doi.org/10.12989/sss.2019.24.2.267
Maranganti, R., Sharma, N.D. and Sharma, P. (2006), "Electromechanical coupling in nonpiezoelectric materials due to nanoscale nonlocal size effects: Green's function solutions and embedded inclusions", *Phys. Rev. B - Condens Matt. Mater. Phys.*, **74**(1), 1-14. https://doi.org/10.1103/PhysRevB.74.014110
Mashkevich, V.S. (1957), "Electrical, optical and elastic properties of diamond type crystals", *Sov. Phys. JETP*, **5**(4), 707-713.
Mehrabadi, S.J., Aragh, B.S., Khoshkhahesh, V. and Taherpour, A. (2012), "Mechanical buckling of nanocomposite rectangular plate reinforced by aligned and straight single-walled carbon nanotubes", *Compos. Part B: Eng.*, **43**(4), 2031-2040. https://doi.org/10.1016/j.compositesb.2012.01.067
Mindlin, R.D. (1968), "Polarization gradient in elastic dielectrics", *Int. J. Solids Struct.*, **4**(6), 637-642. https://doi.org/10.1016/0020-7683(68)90079-6
Minh, P.P. and Duc, N.D. (2019), "The effect of cracks on the stability of the functionally graded plates with variable-thickness using HSDT and phase-field theory", *Compos. Part B: Eng.*, **175**, 107086. https://doi: 10.1016/j.compositesb.2019.107086
Nguyen, T.D., Mao, S., Yeh, Y.-W., Purohit, P.K. and McAlpine, M.C. (2013), "Nanoscale Flexoelectricity", *Adv. Mater.*, **25**(7), 946-974. https://doi.org/10.1002/adma.201203852
Rahmani, O., Hosseini, S.A.H., Ghoytasi, I. and Golmohammadi, H. (2018), "Free vibration of deep curved FG nano-beam based on modified couple stress theory", *Steel Compos. Struct., Int. J.*, **26**(5), 607-620. https://doi.org/10.12989/scs.2018.26.5.607
Robinson, C.R., White, K.W. and Sharma, P. (2012), "Elucidating the mechanism for indentation size-effect in dielectrics", *Appl. Phys. Lett.*, **101**(12), 122901. https://doi.org/10.1063/1.4753799
Salah, F., Boucham, B., Bourada, F., Benzair, A., Bousahla, A.A. and Tounsi, A. (2019), "Investigation of thermal buckling properties of ceramic-metal FGM sandwich plates using 2D integral plate model", *Steel Compos. Struct., Int. J.*, **33**(6), 805-822. https://doi.org/10.12989/scs.2019.33.6.805
Sharma, N.D., Maranganti, R. and Sharma, P. (2007), "On the possibility of piezoelectric nanocomposites without using piezoelectric materials", *J. Mech. Phys. Solids*, **55**(11), 2328-2350. https://doi.org/10.1016/j.jmps.2007.03.016
Sharma, N.D., Landis, C.M. and Sharma, P. (2010), "Piezoelectric thin-film super-lattices without using piezoelectric materials", *J. Appl. Phys.*, **108**(2), 024304. https://doi.org/10.1063/1.3443404
Shen, S. and Hu, S. (2010), "A theory of flexoelectricity with surface effect for elastic dielectrics", *J. Mech. Phys. Solids*, **58**(5), 665-677. https://doi.org/10.1016/j.jmps.2010.03.001
Shu, L., Wei, X., Pang, T., Yao, X. and Wang, C. (2011), "Symmetry of flexoelectric coefficients in crystalline medium", *J. Appl. Phys.*, **110**(10), 104106. https://doi.org/10.1063/1.3662196
Tagantsev, A.K. (1986), "Piezoelectricity and flexoelectricity in crystalline dielectrics", *Phys. Rev. B*, **34**(8), 5883-5889. https://doi.org/10.1103/PhysRevB.34.5883
Tagantsev, A.K. and Gerra, G. (2006), "Interface-induced phenomena in polarization response of ferroelectric thin films", *J. Appl. Phys.*, **100**(5), 051607. https://doi.org/10.1063/1.2337009
Tanner, S.M., Gray, J.M., Rogers, C.T., Bertness, K.A. and Sanford, N.A. (2007), "High-*Q* GaN nanowire resonators and oscillators", *Appl. Phys. Lett.*, **91**(20), 203117. https://doi.org/10.1063/1.2815747
Van Thu, P. and Duc, N.D. (2016), "Non-linear dynamic response and vibration of an imperfect three-phase laminated nanocomposite cylindrical panel resting on elastic foundations in thermal environments", *Sci. Eng. Compos. Mater.*, **24**. https://doi.org/10.1515/secm-2015-0467
Wang, Z.L. (2006), "Piezoelectric Nanogenerators Based on Zinc Oxide Nanowire Arrays", *Science*, **312**(5771), 242-246. https://doi.org/10.1126/science.1124005
Wattanasakulpong, N. and Chaikittiratana, A. (2015), "Exact solutions for static and dynamic analyses of carbon nanotube-reinforced composite plates with Pasternak elastic foundation", *Appl. Mathe. Model.*, **39**(18), 5459-5472. https://doi.org/10.1016/j.apm.2014.12.058
Yang, X.D., Chen, L.Q. and Zu, J.W. (2011), "Vibrations and stability of an axially moving rectangular composite plate", *J. Appl. Mech.*, **78**(1), 011018-011029. https://doi.org/10.1115/1.4002002
Yang, W., Liang, X. and Shen, S. (2015), "Electromechanical responses of piezoelectric nanoplates with flexoelectricity", *Acta Mechanica*, **226**(9), 3097-3110. https://doi.org/10.1007/s00707-015-1373-8
Yazid, M., Heireche, H., Tounsi, A., Bousahla, A.A. and Houari, M.S.A. (2018), "A novel nonlocal refined plate theory for stability response of orthotropic single-layer graphene sheet resting on elastic medium", *Smart Struct. Syst., Int. J.*, **21**(1), 15-21. https://doi.org/10.12989/sss.2018.21.1.015
Yudin, P.V. and Tagantsev, A.K. (2013), "Fundamentals of flexoelectricity in solids", *Nanotechnology*, **24**(43), 432001. https://doi.org/10.1088/0957-4484/24/43/432001
Zhang, Z. and Jiang, L. (2014), "Size effects on electromechanical coupling fields of a bending piezoelectric nanoplate due to surface effects and flexoelectricity", *J. Appl. Phys.*, **116**(13), 134308. https://doi.org/10.1063/1.4897367
Zhang, Z., Yan, Z. and Jiang, L. (2014), "Flexoelectric effect on

the electroelastic responses and vibrational behaviors of a piezoelectric nanoplate", *J. Appl. Phys.*, **116**(1), 014307. https://doi.org/10.1063/1.4886315

Zhang, S., Xu, M., Liu, K. and Shen, S. (2015), "A flexoelectricity effect-based sensor for direct torque measurement", *J. Phys. D: Appl. Phys.*, **48**(48), 485502. https://doi.org/10.1088/0022-3727/48/48/485502

Zhao, M., Qian, C., Lee, S.W.R., Tong, P., Suemasu, H. and Zhang, T.Y. (2007), "Electro-elastic analysis of piezoelectric laminated plates", *Adv. Compos. Mater.*, **16**(1), 63-81. https://doi.org/10.1163/156855107779755273

Zenkour, A.M. (2015), "A comparative study for bending of cross-ply laminated plates resting on elastic foundations", *Smart Struct. Syst, Int. J.*, **15**(6), 1562-1582. https://doi.org/10.12989/sss.2015.15.6.1569

Zhu, P., Lei, Z.X. and Liew, K.M. (2012), "Static and free vibration analyses of carbon nanotube-reinforced composite plates using finite element method with first order shear deformation plate theory", *Compos. Struct.*, **94**(4), 1450-1460. https://doi.org/10.1016/j.compstruct.2011.11.010

Zubko, P., Catalan, G. and Tagantsev, A.K. (2013), "Flexoelectric effect in solids", *Annual Rev. Mater. Res.*, **43**(1), 387-421. https://doi.org/10.1146/annurev-matsci-071312-121634

CC